https://doi.org/10.64989/rmutsbj.2026.268883

Development of bio-based cooking oil-absorbing paper from rice straw fiber, kaffir lime (*Citrus hystrix* DC) fiber, and cassava starch (Cultivar 81)

Pawinee Theamdee*, Gannigar Onsamlee and Pattamaphon Yucharoen

Abstract

This study focused on the development of oil-absorbing paper from bio-based materials using rice straw fiber (RF), kaffir lime fiber (KF), and cassava starch (Cultivar 81) as the main components. The effects of KF incorporation at different proportions (0, 10, 30 and 50% by weight of rice straw) were investigated to evaluate the chemical, physical, mechanical, antimicrobial, and biodegradability properties. All samples were analyzed using FTIR spectroscopy to examine their chemical structures. The results showed a noticeable decrease in signals corresponding to hemicellulose and lignin after alkaline treatment, while the cellulose structure remained evident. Based on the analysis of physical and mechanical properties and oil-absorbing performance, the sample containing 30% KF exhibited the most balanced and optimal performance. This sample showed enhanced oil absorption, high porosity, suitable thickness, and a fibrous structure that facilitated efficient oil uptake, making it particularly suitable for food applications. Furthermore, the inclusion of KF effectively inhibited the growth of *Escherichia coli* (*E. coli*) and *Staphylococcus aureus* (*S. aureus*), with the inhibition zone diameter increasing proportionally with KF content. However, a higher KF content slightly reduced the biodegradation rate, likely due to its antimicrobial properties that suppressed microbial activity in the soil. Overall, incorporating KF into rice straw-based paper significantly improved its oil absorption capacity, mechanical and hydrophobic properties, and antimicrobial activity, without compromising biodegradability. These characteristics highlight its promise as an environmentally sustainable material for oil-absorbing and packaging applications.

Keywords: oil-absorbing paper, rice straw fiber, kaffir lime, cassava starch, bio-based materials, natural fiber

Faculty of Science and Technology, Thepsatri Rajabhat University, Muang District, Lopburi 15000, Thailand

* Corresponding author: E-mail: pawinee.t@lawasri.tru.ac.th

Received: August 21, 2025; Revised: October 30, 2025; Accepted: December 4, 2025

Introduction

In recent years, consumers have become increasingly concerned about health and nutrition, particularly with regard to the consumption of deep-fried foods, which typically contain excessive amounts of residual oil. This excess oil has been associated with various long-term health issues (Ferdian et al., 2023). Consequently, the development of efficient oil-absorbing materials for fried foods has emerged as a promising strategy to promote healthier food products and meet the demands of health-conscious consumers (Ferdian et al., 2023; Zhang et al., 2023). Currently, most commercially available oil-absorbent paper is produced from hardwood pulp. The use of wood as a primary raw material directly contributes to environmental degradation, as the trees required for paper production have long growth cycles and the harvesting process accelerates deforestation (Yimlamai et al., 2024). Global trends toward sustainable development have encouraged the utilization of natural, renewable, and biodegradable raw materials, particularly plant-based fibers, which play a significant role in modern paper production (Yimlamai et al., 2024). Agricultural waste materials such as loofah fiber (Xing et al., 2024), maize stalk fibers (Risa & Wolla, 2025), water hyacinth (Wichianphong & Maison, 2020; Wembe et al., 2023), pineapple leaves (Bakti et al., 2025), banana fiber (Chattaviriya et al., 2022), corn husk, and sugarcane bagasse fiber (Bhardwaj et al., 2023) have received growing attention as alternative fiber sources to wood pulp due to their abundance, low cost, and environmental friendliness.

Previous studies (Wang et al., 2022; Boonmahitthisud et al., 2023) have indicated that oil-absorbing paper materials are typically evaluated based on their oil absorption capacity, porosity, the balance between hydrophobicity and water permeability, and surface roughness, all of which directly affect the dynamics of oil retention and absorption. However, research on developing bio-based oil-absorbing paper that combines natural antimicrobial properties while maintaining biodegradability remains limited. Moreover, there is a lack of data on the optimal proportion of natural binders or reinforcing phases that can enhance the paper's absorption efficiency and mechanical strength.

The Mahasorn community, located in Ban Mi District, Lopburi Province, is rich in agricultural resources, including medicinal and aromatic plants such as kaffir lime (*Citrus hystrix* DC). Juice extraction generates substantial residues of peel and fibrous components, with the peel containing oil glands rich in bioactive compounds, including β-pinene, citronellal, and terpinen-4-ol, which exhibit antimicrobial properties (Abirami et al., 2014; Budiarto et al., 2024). However, the limited fiber content of kaffir lime residues alone is insufficient for paper formation, resulting in low mechanical strength. To address this, additional plant-based fibers such as rice straw—an abundant by-product of local rice cultivation, typically used as animal feed or fertilizer, can be incorporated to enhance the fiber content for value-added applications. Rice straw (RS) is a holocellulose-rich (cellulose+hemicellulose) lignocellulose waste (Malik et al., 2023) composed of cellulose (40-50%), hemicellulose (25-35%), and lignin (15-20%) (Serrano-Martínez et al., 2024). Various applications of rice straw (RS) have been proposed, including the extraction of bioactive compounds (Hillscher et al., 2024), biodiesel synthesis (Sahu, 2021), and paper production (Nagpal et al., 2021; Hillscher et al., 2024). Therefore, the management of agricultural waste, particularly

rice straw, is urgently needed to address the ongoing issue of open-field burning. Paper has great potential to be produced from non-wood lignocellulosic biomass. Additionally, the strength properties of paper need to be improved to meet market demands. In this context, our approach involves adding dry strength additives, such as starch (CS) and carboxymethyl cellulose (CMC), to the cellulosic pulp to improve its strength and surface properties (Islam et al., 2024). Nevertheless, starch is a more suitable bio-additive for hand sheet packaging paper, offering improved surface and mechanical properties. To address strength limitations, a natural binder such as cassava starch (Cultivar 81) is incorporated. This starch is locally available, cost-effective, and composed of key constituents, including amylose (17-24%) and amylopectin (76-83%) (Das et al., 2024), which provide adhesive properties that enhance the mechanical integrity of the final paper product. Bamisaye & Rapheal (2023) investigated the effect of cassava starch binder type on the properties of briquettes produced from NaOH-treated banana leaves. The study found that briquettes using cassava starch as a binder exhibited superior quality and improved physicochemical properties compared to those using other types of binders.

Therefore, the objectives of this study were clearly defined as follows: (1) to develop bio-based oil-absorbing paper using rice straw fiber, kaffir lime fiber, and cassava starch (Cultivar 81) as the main components; (2) to evaluate the effect of varying kaffir lime content on the physical, mechanical, and oil-absorbing properties of the paper; and (3) to examine the antimicrobial and biodegradability performance to ensure functionality and environmental compatibility. The physical properties assessed included thickness, water activity (a_w), color values, water solubility, water absorption, oil absorption, and vertical oil absorption. Chemical characteristics were examined using Fourier-transform infrared spectroscopy (FTIR), and mechanical properties were evaluated through puncture resistance and shear strength tests. Additionally, the antimicrobial activity of the samples and the biodegradability of the oil-absorbent paper were investigated to assess their suitability as environmentally friendly materials.

Methodology

1. Materials

Cassava tubers (Cultivar 81) with uniform size and shape, kaffir lime residues from juice extraction, and rice straw were sourced from the Mahasorn community, Ban Mi District, Lopburi Province, Thailand. All reagents and chemicals, including sodium hydroxide (NaOH) and hydrogen peroxide (H_2O_2, 50%v/v), were of technical grade. *Staphylococcus aureus* (TISTR 51) and *Escherichia coli* (TISTR 887) were employed as test organisms. These bacteria were cultured on Muller–Hinton agar (Merck, Germany).

2. Preparation of kaffir lime fiber (KF)

Kaffir lime residues were first washed thoroughly and then dried in a hot air oven at 60°C for 24h. The dried residues were subsequently ground and sieved to obtain a fine powder with a particle size of approximately 100-150μm, which was then stored in a desiccator until further use (Ying et al., 2023).

3. Preparation of rice straw fiber (RF)

The alkali treatment procedure was adapted from the method of Harun & Geok (2016). Rice straw was air-dried at ambient temperature for one week to reduce the moisture content to below 15%, then cut into

pieces of approximately 3-5cm. A 500g portion of the straw was soaked in a 5% (w/v) NaOH solution at a biomass-to-solution ratio of 1:20 (w/v) for 2h at 55°C. After soaking, the rice straw was separated from the solution by cloth filtration and washed thoroughly with clean water until the slimy texture disappeared, indicating the removal of residual chemicals. The cleaned fibers were soaked in a 25% v/v hydrogen peroxide solution for 1h to facilitate bleaching and further removal of impurities. After each bleaching step, the fibers were rinsed with distilled water and filtered to remove residual solution. Finally, the fibers were oven-dried at 60°C for at least 24h, placed in a sealed container, and stored in a desiccator for further use (Freitas et al., 2024).

4. Preparation of cassava starch (Cultivar 81) (CS)

The method for extracting cassava starch was adapted from the procedure described by Elisabeth et al., (2022). Fresh cassava tubers (Cultivar 81) were selected, peeled, washed, and soaked in water for approximately 20 minutes to reduce cyanogenic compounds. The tubers were then cut into small slices (3- 5mm thick). Each portion was blended using an electric blender until finely ground to obtain a uniform pulp. The pulp was filtered through a muslin cloth to remove fibrous residues. The filtrate was then left to stand undisturbed, allowing the starch to precipitate naturally. The sedimented starch was collected and washed twice with distilled water to remove impurities. It was subsequently dried in a hot-air oven at 60°C for 24h. Finally, the dried starch was ground using a flour mill, sieved through a 100-mesh screen, and stored in a sealed container inside a desiccator for later use.

5. Paper sheet preparation

Modified from the method described by Toro et al., (2020). Paper sheets were formed by mixing rice straw fiber (RF), kaffir lime fiber (KF), and cassava starch (CS). The ratio of RF was kept constant at 20g for all samples, while the KF was varied at 0% (RS-KF0), 10% (RS-KF10), 30% (RS-KF30), and 50% (RS-KF50) by weight of rice straw. The CS was maintained at 2g for all samples as a natural binder. The mixture was diluted with 1L of water and blended for 2min to ensure homogeneity. The resulting pulp slurry was poured into a wooden frame mold (20×30cm) and evenly spread to form uniform sheets. The wet sheets were air-dried for 24h, then carefully removed from the mesh to prevent damage (Figure 1). The dried paper sheets were stored in sealed containers and kept in a desiccator before analysis. The obtained samples were subsequently compared with commercial oil-absorbing paper, which served as the control.

6. Characterizations

FTIR

FTIR measurements were performed using an FTIR spectrometer (Perkin Elmer, Spectrum 100 FTIR System Universal, USA) equipped with a diamond-cell attenuated total reflectance (ATR) sampling accessory. The spectra were collected as the average of at least 32 scans at a resolution of 4cm^{-1} in the frequency range of 4,000-400cm^{-1} for the spectroscopic analysis of the samples.

7. Thickness

The thickness of the paper sheets was measured using a digital micrometer (Mitutoyo, Japan) at five random positions, and the average value was reported in millimeters (mm).

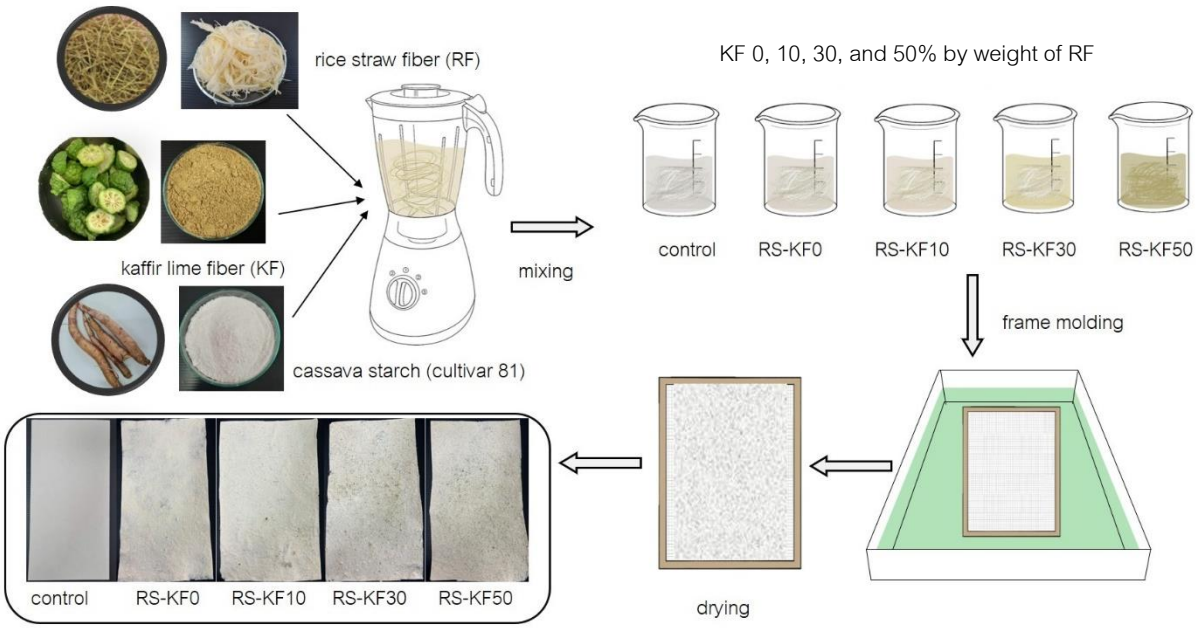

Figure 1 Representative schematic of the production of oil-absorbing paper from rice straw fiber (RF), kaffir lime fiber (KF), and cassava starch (Cultivar 81).

8. Water activity (a_w)

The water activity (a_w) of the paper samples was directly measured at room temperature using a water activity meter (Aqualab 4TE, USA) to determine the moisture availability and assess the potential for microbial growth. Each sample was analyzed in triplicate, and the mean value was reported. According to general guidelines, samples with a_w values above 0.8 are considered susceptible to microbial growth (Sun et al., 2023).

9. Color properties

The color properties (L^*, a^*, and b^* values) of the film samples were measured using a colorimeter (Color-Flex EZ, HunterLab, Thailand) based on the CIELAB color system. The lightness value (L^*) varies from 0, representing black, to 100, representing white. The a^* axis indicates color from green ($-a^*$) to red ($+a^*$), while the b^* axis represents color from blue ($-b^*$) to yellow ($+b^*$) (Kirillova et al., 2015). The film samples were cut into pieces of 1.50×1.50cm, and color measurements were taken at three different positions per sheet. Three replicate sheets were analyzed for each sample, and the mean values were reported.

10. Water solubility (WS)

WS (%) was determined using a modified method based on Paudel et al., (2022). Film samples were cut into squares of 2×2cm. The initial dry weight (W_i) of each sample was recorded. The samples were then immersed in distilled water at 25°C and shaken using a mechanical shaker for 1h. After immersion, the remaining solid samples were dried in a hot air oven at 105°C for 1h and then weighed again (W_f). The test was performed in triplicate, and the water solubility percentage was calculated using Equation (1) (Paudel et al., 2022).

$$WS(\%) = \frac{W_i - W_f}{W_i} \times 100 \quad (1)$$

11. Water absorption (WA)

WA (%) was measured using a modified method based on Zaafarani et al., (2024). Film samples were cut into 2.0×2.0cm pieces. Before testing, the initial weight and dimensions of each sample were recorded (W_d). The samples were then immersed in 100mL of distilled water at 25°C for 1h. After immersion, the new weight of the water-absorbed samples was recorded (W_w). The test was performed in triplicate, and the percentage of water absorption was calculated using Equation (2) (Zaafarani et al., 2024).

$$WA(\%) = \frac{W_w - W_d}{W_d} \times 100 \quad (2)$$

12. Vertical oil absorption

Oil absorption was measured using a modified method based on Barthlott et al., (2020). The vertical oil absorption test was carried out to evaluate the oil uptake capacity of the samples under gravity-driven conditions. Three types of oil with different viscosities, namely lard, palm oil, and soybean oil, were selected for the test, representing commonly used oils relevant to practical applications. The samples were cut into standard rectangular sizes (2 ×5 cm) and suspended vertically with the bottom edge immersed in the oil. The time was recorded until the oil fully penetrated and reached the top of the sample. The test was conducted in triplicate, and the average values were reported.

13. Oil absorption test

The oil absorption test was adapted from the method described by Maimaiti et al., (2014). Paper samples were cut into 5×5cm pieces and placed horizontally on white paper, with a 2g heap of sand positioned at the center to simulate localized pressure. Subsequently, 1mL of oil was dropped directly onto the sand heap, and the time was recorded from the moment the oil was applied until it visibly penetrated through the paper sheet. Each type of oil (lard, palm oil, and soybean oil) was tested in triplicate, and the average penetration time was reported as an indicator of oil absorption performance.

14. Mechanical properties

Puncture and tear strength were evaluated using a texture analyzer (Stable Microsystems, TA-XT2, UK), with slight modifications to the testing procedure described by Liu et al., (2022). For the puncture strength test, an HDP/CFS probe in combination with the heavy-duty platform was used. The samples were cut into 2.50×2.50cm pieces and tested at a probe speed of 5 mm/s until the probe fully penetrated the sample. For the tear strength test, a Craft Knife Adaptor & Blades (A/CKB) was used along with the HDP/90 platform. The samples were cut into 6×9cm pieces and tested at a probe speed of 1mm/s with a penetration distance of 4mm through the sample. Each test was performed in triplicate, and the average values were reported.

15. Antimicrobial activity

The antimicrobial activity of the samples was evaluated using the agar diffusion method, as modified from Ketkaew et al., (2017); Hosseini et al., (2009). Two foodborne pathogenic bacteria, *Escherichia coli* (*E. coli*)

and *Staphylococcus aureus* (*S. aureus*), were selected as representative strains. The bacterial cultures were incubated overnight at 37°C, then diluted to a turbidity equivalent to the McFarland standard 0.5 (approximately 10^8CFU/mL). The suspensions were inoculated onto Mueller-Hinton agar plates using the swab plate technique. Sterilized sample discs (6mm in diameter) were placed on the inoculated plates and incubated at 37°C for 24h. Each formulation was tested in triplicate using three discs per sample. Bacterial growth inhibition was indicated by the clear zone surrounding each disc, and the inhibition zone diameter was measured in mm.

16. Biodegradation test

The biodegradability of the samples was evaluated using the soil burial method in loamy soil, with modifications based on the method of Paudel et al., (2022). The samples were first oven-dried at 105°C for 24h, and the initial dry weight (W_0) was recorded. Three replicates of each formulation were prepared, with three samples per replicate, and were vertically buried in the soil at a depth of approximately 10-12cm from the soil surface, inside high-density polyethylene boxes filled with soil. The boxes were incubated at a constant temperature of 33±2°C for 8 weeks. The initial soil moisture content was adjusted to approximately 35%, with no additional watering during the test period. Each week, the samples were carefully removed from the soil, and any adhering soil was gently cleaned by hand. The samples were then oven-dried again at 105°C for 24h, and the final dry weight (W_t) was recorded. The percentage of weight loss was calculated according to Equation (3) (Paudel et al., 2022).

$$Weighloss(\%) = \frac{W_0 - W_t}{W_0} \times 100 \quad (3)$$

17. Statistical analysis

Statistical analysis was performed using SPSS® Version 12 (SPSS Inc., USA). The mean values obtained from the tests were compared using one-way analysis of variance (ANOVA), and differences between treatment groups were determined using Duncan's multiple range test (DMRT) at a significance level of $p \leq 0.05$.

Results and discussion

1. FTIR

(Figures 2a-b) present the infrared spectra of RF before and after alkali treatment. A broad absorption peak around 3,295cm^{-1} corresponds to the O–H stretching vibration of hydroxyl groups. After alkali treatment, the intensity of this peak was noticeably reduced, indicating a decrease in the hydroxyl group content. Additionally, a peak near 1,700cm^{-1}, attributed to the C=O stretching vibration of acetyl and carboxyl groups in hemicellulose, also showed a marked reduction in intensity in the treated fibers. Similarly, the C–O stretching vibration peaks associated with lignin and hemicellulose at approximately 1,250 and 1,033cm^{-1}, respectively, were significantly diminished. These reductions suggest a partial removal of lignin and hemicellulose components from the rice straw fiber structure following alkali treatment, which is consistent with the findings reported by Yang et al., (2023). (Figure 2c) displays the characteristic absorption bands of CS. A broad band observed around 3,300cm^{-1}

corresponds to the O–H stretching vibration of hydroxyl groups in amylose and amylopectin. A peak near 2,933cm^{-1} is associated with the C–H stretching, while the side chain CH_2–OH bending vibration appears at approximately 1,337cm^{-1}. The stretching vibrations of C–O and C–C bonds are observed at 1,150 and 1,077cm^{-1}, respectively. Additionally, the strong absorption band at 1,000cm^{-1} is attributed to the bending vibration of the C–O–H group, which is consistent with the findings reported by Rahaman et al., (2021). (Figure 2d) presents the FTIR spectral peaks of KF. The broad absorption band at 3,307cm^{-1} corresponds to the O–H stretching vibration, indicating the presence of phenolic compounds such as terpinen-4-ol, and citronellol (Ying et al., 2023; Malikhah & Herdyastuti, 2023). The absorption peak observed at 1,721cm^{-1} is attributed to the C=O stretching vibration, which may arise from the presence of aldehyde, ester, carboxylic acid, or ketone functional groups (Malikhah & Herdyastuti, 2023; Ramadhan et al., 2018). Additionally, the peak at 1,620cm^{-1} corresponds to the C=C stretching of aromatic rings, suggesting the presence of terpene or terpenoid compounds, such as citronellal (Malikhah & Herdyastuti, 2023). The incorporation of increasing amounts of kaffir lime fiber into the formulation resulted in noticeable changes in the FTIR spectra, as shown in (Figures 2e-h). Specifically, the absorbance intensities of the O-H, C=O, and C=C functional groups increased, indicating a higher presence of carbonyl and unsaturated compounds associated with KF components.

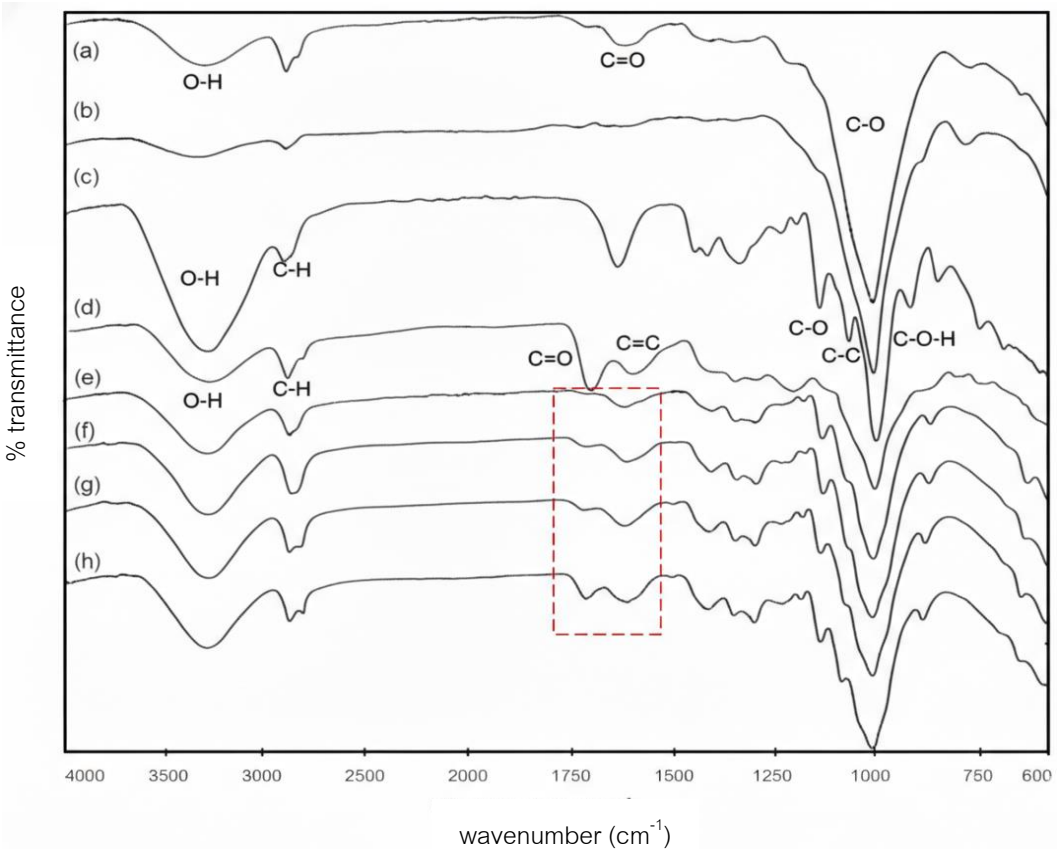

Figure 2 FTIR spectra of RF before alkali treatment (a), RF after alkali treatment (b), CS (c), KF (d), RS-KF0 (e), RS-KF10 (f), RS-KF30 (g) and RS-KF50 (h).

2. Physical appearance

As shown in (Figure 3), the physical appearance of the formed paper sheets varied with increasing amounts of KF. The RS-KF0 sample appeared thin, easily torn, and relatively smooth. In contrast, RS-KF10 exhibited a rougher surface texture and greater thickness. RS-KF30 and RS-KF50 displayed noticeably rougher surfaces, along with thicker and stiffer structures. Compared to the commercial oil-absorbing paper (control), which had a smooth, thin, and uniform texture, the KF-containing samples showed substantial differences in their physical characteristics.

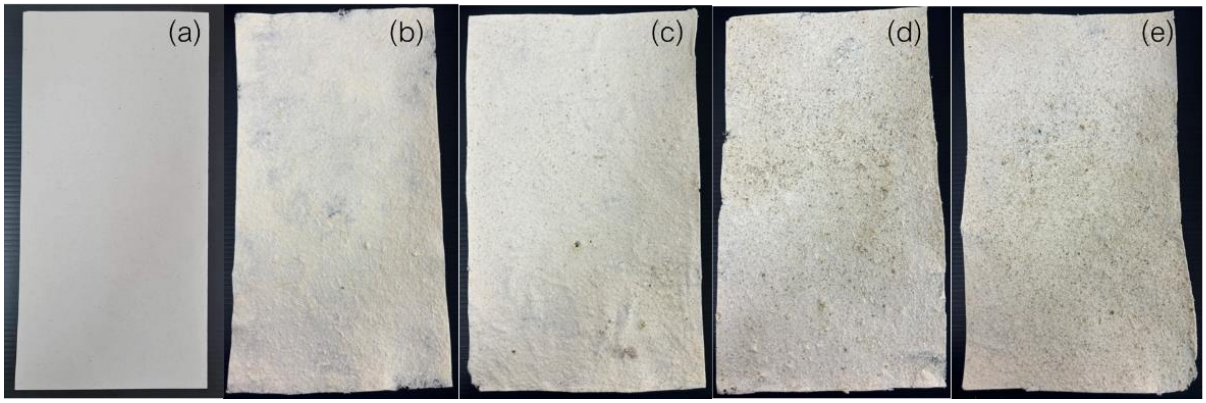

Figure 3 The appearance of paper sheets compared with commercial oil-absorbing paper (control) (a), RS-KF0 (b), RS-KF10 (c), RS-KF30 (d), and RS-KF50 (e).

3. Thickness

(Table 1) presents the thickness of the paper sheets. The trend suggests that increasing KF content enhanced fiber compactness ($p \leq 0.05$), resulting in thicker paper structures compared to the commercial oil-absorbing paper (control).

4. Water activity (a_w)

The a_w values (Table 1) of the paper sheets ranged from 0.45-0.37, which were lower than those of the commercial oil-absorbing paper. The significant decrease ($p \leq 0.05$) in a_w with increasing KF content may be attributed to the hydrophobic nature of KF, which contains peel and fiber components with functional groups that are likely to inhibit the interaction between cellulose and water molecules. Consequently, the water retention capacity of the paper sheets was reduced. Moreover, a_w values below 0.60 are considered safe for storage, as they can inhibit the growth of undesirable microorganisms such as molds and yeasts (Ray et al., 2022). This suggests that the developed paper sheets are microbiologically safe and have improved product shelf stability.

5. Color properties

(Table 1) presents the color parameters (L^*, a^* and b^*) of the paper sheets. The color parameters of the paper sheets revealed that the L^* values, which indicate lightness, ranged from 78.01-79.65 and showed a decreasing ($p \leq 0.05$) trend with increasing KF content. This reduction in brightness is likely due to the brownish-

yellow color of KF. In contrast, the a^* and b^* values, representing the red-green and yellow-blue color axes, respectively, increased ($p \leq 0.05$) with higher KF content. This is consistent with the visual appearance of the paper sheets, which exhibited a reddish-yellow hue corresponding to the increasing amounts of KF in the formulation. The observed hue is attributed to the natural pigments and phenolic compounds present in the kaffir lime peel, particularly flavonoids, carotenoids, and tannins, which determine the color. Additionally, partial oxidation of tannins during the drying process may produce brown-colored compounds, enhancing the overall color intensity. Therefore, increasing the KF content in the formulation resulted in progressively more pronounced reddish-yellow paper sheets.

Table 1 Physical properties of the paper sheets that varied with increasing amounts of KF.

sample	thickness (mm)	a_w	color		
			L^*	a^*	b^*
control	0.08±0.01^{e}	0.45±0.00^{a}	78.01±0.70^{e}	0.09±0.01^{b}	1.35±0.02^{e}
RS-KF0	0.11±0.01^{d}	0.43±0.01^{b}	87.08±0.60^{a}	-0.34±0.08^{d}	10.53±0.11^{d}
RS-KF10	0.13±0.01^{c}	0.41±0.01^{c}	83.84±0.32^{b}	-0.21±0.11^{c}	11.68±0.85^{c}
RS-KF30	0.15±0.01^{b}	0.39+0.01^{d}	82.76+0.57^{c}	0.03+0.01^{b}	13.21±0.72^{b}
RS-KF50	0.17±0.01^{a}	0.37±0.01^{d}	79.65±0.45^{d}	0.26±0.05^{a}	15.83±0.64^{a}

$^{a-e}$ values are presented as mean±standard deviation. different superscript letters within the same column indicate a statistically significant difference ($p \leq 0.05$).

6. Water solubility (WS) and water absorption (WA)

The Water solubility (WS) and water absorption (WA) values of the paper sheets varied with increasing amounts of KF, as presented in (Table 2). Both parameters are critical indicators for evaluating the stability and quality of products under high-humidity conditions. The results revealed that WS and WA values tended to decrease ($p \leq 0.05$) with the increased incorporation of KF in the paper formulation. This may be attributed to the composition of KF, which includes peel and fibrous materials possessing hydrophobic properties. Additionally, KF acts as a filler that fills the voids within the fiber matrix, resulting in a denser paper structure that limits water penetration. Moreover, the compounds present in KF likely reduce the ability of cellulose to bind with water molecules by decreasing hydrogen bond formation between cellulose and water (Bharti et al., 2022; Mazega et al., 2022). Consequently, the paper sheets exhibited reduced water absorption compared to the commercial oil-absorbing paper (control), which showed higher WS and WA values, although still lower than those of the RS-KF0 sample.

Table 2 Water solubility (WS) and water absorption (WA) of the paper sheets that varied with increasing amounts of KF.

sample	WS (%)	WA (%)
control	11.89+0.60[a]	760.47+10.54[b]
RS-KF0	12.72+1.97[a]	873.81+15.96[a]
RS-KF10	11.44+2.64[a]	709.01+28.02[c]
RS-KF30	8.23+1.01[b]	613.63+21.56[d]
RS-KF50	5.00+0.79[c]	585.09+25.10[d]

[a-d] values are presented as mean±standard deviation. different superscript letters within the same column indicate a statistically significant difference ($p \leq 0.05$).

7. Vertical oil absorption and oil absorption

The vertical oil absorption of the paper sheets tested with three types of oil, soybean oil, palm oil, and lard, is presented as average penetration time in (Table 3). The results indicated that the vertical oil absorption capacity tended to increase ($p \leq 0.05$) with higher amounts of KF incorporated into the formulation, as evidenced by the shorter absorption time. This enhancement may be attributed to the porous structure of the paper (Wu et al., 2025) and the fibrous components of KF, which contribute to an increased surface area for oil absorption. When comparing the absorption efficiency among the different types of oil, the paper sheets exhibited the highest absorption capacity for soybean oil, followed by palm oil and lard, respectively. This trend may be associated with the viscosity and surface tension of the oils; soybean oil has a lower viscosity and surface tension than palm oil and lard (Qi et al., 2019), thereby facilitating easier penetration and movement through the paper matrix. This observation is consistent with the findings of Baethlott et al., (2020), which demonstrated that as the viscosity of the oil increases, the vertical transport velocity of the oil on the surface decreases. This is consistent with the oil absorption results, as shown by the average penetration time in (Table 3), indicating that the paper sheets absorbed oil more rapidly ($p \leq 0.05$) with increasing amounts of KF in the formulation. This improvement may be attributed to the higher fiber density per unit area, which reduces the void spaces between fibers and thus facilitates faster oil penetration. These findings align with the study by Xu et al., (2015), which reported that water and oil can be absorbed into double-twisted ropes *via* capillary action through small voids and grooves within the fibrous structure. Furthermore, when comparing the absorption efficiency among the three types of oil, the paper sheets exhibited the fastest absorption for soybean oil, followed by palm oil and lard, respectively. This trend may be explained by the lower viscosity of soybean oil, which reduces resistance to flow into the porous structure of the paper, thereby allowing more efficient infiltration and faster absorption compared to oils with higher viscosity. When comparing oil absorption performance, paper containing KF demonstrated superior oil absorption capacity compared to other natural or cellulose-based oil-absorbing materials, such as coconut shell. The coconut shell, when ground into powder, exhibits irregular particle shapes, and the strong interfacial adhesion between fibers and the matrix further limits oil penetration (Rosdi et al., 2022), resulting in lower oil absorption than KF-based paper.

Table 3 The vertical oil absorption performance and oil absorption test of the paper sheets at various KF ratios.

sample	vertical oil absorption			oil absorption		
	soybean oil (min)	palm oil (min)	lard (min)	soybean oil (min)	palm oil (min)	lard (min)
control	42.67±1.15^{a}	45.67±1.15^{a}	52.33±2.52^{a}	27.67±1.53^{a}	32.31±1.53^{a}	35.00±1.10^{a}
RS-KF0	17.00±1.73^{b}	17.33±1.13^{b}	20.00±2.65^{b}	18.00±1.00^{b}	18.23±1.15^{b}	19.67±1.15^{b}
RS-KF10	13.67±1.15^{c}	14.42±1.20^{c}	16.27±1.53^{c}	15.33±1.15^{c}	16.00±1.00^{c}	17.33±1.25^{c}
RS-KF30	10.33±0.58^{d}	11.67±1.24^{d}	14.34±0.58^{c}	12.67±0.58^{d}	14.12±1.21^{cd}	15.00±1.30^{d}
RS-KF50	8.67±0.58^{d}	10.32±1.33^{d}	10.51±0.57^{d}	11.12±0.45^{d}	12.33±1.17^{d}	13.13±1.07^{d}

$^{a-d}$ values are presented as mean±standard deviation. different superscript letters within the same column indicate a statistically significant difference ($p \leq 0.05$).

8. Mechanical properties

The analysis of puncture strength and tear strength of the paper sheets, as presented in (Table 4), revealed that both properties tended to increase ($p \leq 0.05$) with higher amounts of KF incorporated into the formulation. This improvement may be attributed to the fibrous components of KF acting as reinforcing agents within the paper matrix, enhancing the structural integrity and inter-fiber bonding (Rangappa et al., 2022). As a result, the paper sheets exhibited greater resistance to puncture and tearing strength. In comparison with commercial oil-absorbing paper (control), all KF-based sheets demonstrated superior mechanical properties, as the commercial paper exhibited the lowest puncture and tear strength values. This highlights the reinforcing potential of KF in improving the durability of the developed paper sheets. This is consistent with the study by Todorova et al., (2022), which found that the tear index of base paper is lower than that of paper treated with lavender oil. This improvement is attributed to the enhanced bonding ability of the cellulose fibers. Despite the increased moisture from the essential oil treatment, the fibers maintained strong inter-fiber bonds, resulting in increased tear resistance of the paper after treatment.

Table 4 Mechanical properties of the paper sheets at various KF ratios.

sample	puncture strength (N/m^2)	tear strength (N/m^2)
control	1.43±0.14^{c}	46.42±2.98^{d}
RS-KF0	1.46±0.20^{c}	53.69±4.77^{c}
RS-KF10	2.09±0.25^{b}	86.11±3.03^{b}
RS-KF30	2.32±0.14^{b}	128.96±2.26^{a}
RS-KF50	5.13±0.17^{a}	131.43±3.11^{a}

$^{a-d}$ values are presented as mean±standard deviation. different superscript letters within the same column indicate a statistically significant difference ($p \leq 0.05$).

9. Antimicrobial activity

The results of the antimicrobial activity test for samples containing increasing amounts of KF against *E. coli* and *S. aureus* are presented in (Table 5). The antibacterial test showed that inhibition zones were observed in samples RS-KF10, RS-KF30, and RS-KF50, with the diameter of the zones increasing proportionally ($p \leq 0.05$) with the KF content. In contrast, the samples without KF (RS-KF0) and the commercial oil-absorbing paper (control) exhibited no inhibitory effect. Notably, the inhibition zones for *S. aureus* were generally larger than those for *E. coli* at the same KF concentration, indicating that *S. aureus* is more sensitive to the antimicrobial components of KF. This difference can be attributed to the structural characteristics of the bacterial cell walls: *S. aureus*, a Gram-positive bacterium, has a thicker peptidoglycan layer but lacks the outer membrane present in Gram-negative *E. coli*, allowing terpenoid compounds in KF to more easily penetrate and disrupt cellular structures. These findings are consistent with the report by Rahayu et al., (2024), which indicated that the diameter of the microbial inhibition zone tended to increase with higher extract concentrations, indicating a positive correlation between the amount of extract and its antimicrobial efficacy. The antimicrobial activity of KF is attributed to its terpenoid components, which interact with proteins in the bacterial cell membrane and mitochondria. These interactions form polymeric bonds that disrupt protein structures, reduce membrane permeability, and ultimately lead to nutrient leakage and bacterial cell death. Therefore, the KF-containing paper exhibits selective antimicrobial effects depending on the bacterial strain, which is relevant for applications in food packaging and hygiene-sensitive materials.

Table 5 Diameter of inhibition zones for *E. coli* and *S. aureus*.

microorganism	diameter of inhibition zone (mm)				
	control	RS-KF0	RS-KF10	RS-KF30	RS-KF50
E. coli	NI	NI	0.70 ± 0.02^{c}	13.00 ± 0.13^{b}	20.00 ± 0.17^{a}
S. aureus	NI	NI	0.85 ± 0.10^{c}	15.00 ± 0.15^{b}	24.00 ± 0.20^{a}

$^{a-b}$ values are presented as mean diameter of inhibition zones±standard deviation. different superscripts within the same row indicate a statistically significant difference ($p \leq 0.05$). mm=millimeter, NI=no inhibition.

10. Biodegradation

The weight loss of paper sheets with varying proportions of KF during an 8-week soil burial test reflects the biodegradation process influenced by moisture and microorganisms in the soil. As shown in (Table 6), the degradation rate of the paper sheets tended to decrease ($p \leq 0.05$) as the KF content increased, indicating that the KF content hinders the penetration of water and microorganisms due to its hydrophobic properties (consistent with the results in (Table 2)), thereby reducing the biodegradation rate. Furthermore, it should be noted that KF contains bioactive compounds that affect soil microorganisms by inhibiting spore germination and microbial growth (Ketkaew et al., 2017). In contrast, commercial oil-absorbing paper (control) exhibited a higher degradation rate due to the absence of antimicrobial properties, allowing soil microorganisms to proliferate and accelerate the biodegradation process.

Table 6 Biodegradability and weight loss (%) of the paper sheets at various KF ratios.

time (week)	physical appearance					weight loss (%)
	sample					
	control	RS-KF0	RS-KF10	RS-KF30	RS-KF50	
0						27.76±4.81[a]
2						13.26±4.47[b]
4						9.40±1.45[bc]
6						5.56±0.31[cd]
8						2.95±1.53[e]

[a-e] values are presented as the mean±standard deviation. different superscript letters within the same column indicate a statistically significant difference ($p \leq 0.05$).

Conclusion

This study aimed to develop oil-absorbing paper for fried foods using rice straw fiber, kaffir lime fiber (KF), and cassava starch (Cultivar 81). The effects of KF incorporation at different proportions, 0, 10, 30, and 50% by weight of rice straw, on the chemical, physical, mechanical, antimicrobial, and biodegradation properties were systematically evaluated. Cassava starch (Cultivar 81) was successfully prepared for use in the formulation; however, its yield and compositional properties (fiber, amylose, and amylopectin contents) were not analyzed in this study and will be investigated in future research to enhance data accuracy and completeness. FTIR spectral analysis revealed that cellulose remained intact after alkaline treatment, while signals associated with hemicellulose and lignin decreased. The presence of KF in the paper samples was detected and found to increase proportionally with the added amount. The formulation containing 30% KF demonstrated the most suitable properties for food-contact oil-absorbing paper. Specifically, it exhibited optimal water solubility, water absorption, oil absorption, and vertical oil penetration, indicating effective oil uptake and retention. In particular, the incorporation of 30% KF increased the average oil absorption by approximately 34% and reduced water absorption by around 33% compared to the KF-free sample. Mechanically, the paper formulation maintained puncture resistance and shear strength, with the incorporation of 30% KF increasing the puncture strength by approximately 62.20% and the tear strength by about 177.80% compared to the KF-free sample. Antimicrobial tests showed that 30% KF effectively inhibited *E. coli* and *S. aureus*, with observable inhibition zones, whereas the KF-free sample and commercial paper showed no antimicrobial activity. Biodegradation tests indicated that the degradation rate slightly decreased with KF addition, likely due to the antimicrobial activity of KF inhibiting soil microorganisms responsible for decomposition. Overall, the 30% KF paper meets key performance criteria for oil-absorbing food packaging, combining effective oil absorption, antimicrobial functionality, and environmental degradability. These findings suggest that KF-based bio-paper not only provides an eco-friendly alternative for

oil absorption but also paves the way for the sustainable utilization of agricultural waste in advanced packaging applications. Further work will focus on evaluating long-term storage stability, the influence of food types and temperatures on oil absorption, and the potential migration of bioactive compounds to ensure safety and compliance with food packaging standards.

Acknowledgement

The authors gratefully acknowledge the financial support from the Science, Research, and Innovation Fund (Fundamental Fund, Fiscal Year 2025) under Grant Agreement No. 06/2025, provided through the Research and Development Institute, Thepsatri Rajabhat University, Thailand. The experimental work was conducted at Thepsatri Rajabhat University, Lopburi, Thailand, between March 2024 and February 2025.

References

Abirami, A., Nagarani, G., & Siddhuraju, P. (2014). The medicinal and nutritional role of underutilized citrus fruit Citrus hystrix (Kaffir lime): A review. *Drug Invention Today, 6*(1), 1-5. https://www.researchgate.net/publication/303227547_The_medicinal_and_nutritional_role_of_underutilized_citrus_fruit_Citrus_hystrix_Kaffir_lime_a_review

Bakti, N. S. H. M., Yeu, L. C., Hui, W. Q., Rahmat, A., Hashim, N. F. B. M., Zakri, T. S. A. T., & Asman, S. (2025). Sustainable paper production using treated pineapple leaf fiber and wastepaper composites. *Journal of Science and Technology*, *17*(1), 130-142. https://doi.org/10.30880/jst.2025.17.01.013

Bamisaye, A., & Rapheal, I. A. (2023). Effect of binder type on the NaOH treated briquettes produced from banana leaves. *Biomass Conversion and Biorefinery, 13*(10), 8939-8947. https://doi.org/10.1007/s13399-021-01771-9

Barthlott, W., Moosmann, M., Noll, I., Akdere, M., Wagner, J., Roling, N., Koepchen Thomä, L., Azad, M. A. K., Klopp, K., Gries, T., & Mail, M. (2020). Adsorption and superficial transport of oil on biological and bionic superhydrophobic surfaces: A novel technique for oil–water separation. *Philosophical Transactions of the Royal Society A*, *378*(2167), 20190447. https://doi.org/10.1098/rsta.2019.0447

Bhardwaj, A., Sharma, N., Alam, T., Sharma, V., Sahu, J. K., Hamid, H., Bansal, V., & Alam, M. S. (2023). Development and characterization of chitosan and beeswax–chitosan coated biodegradable corn husk and sugarcane bagasse based cellulose paper. *Waste and Biomass Valorization*, *14*(5), 1625-1636. https://doi.org/10.1007/s12649-022-01952-1

Bharti, S. K., Pathak, V., Alam, T., Arya, A., Singh, V. K., Verma, A. K., & Rajkumar, V. (2022). Starch bio-based composite active edible film functionalized with Carum carvi L. essential oil: Antimicrobial, rheological, physic-mechanical and optical attributes. *Journal of Food Science and Technology*, *59*(2), 456-466. https://doi.org/10.1007/s13197-021-05028-1

Boonmahitthisud, A., Booranapunpong, C., Pattaradechakul, C., & Tanpichai, S. (2023). Development of water-resistant paper using chitosan and plant-based wax extracted from banana leaves. *International Journal of Biological Macromolecules*, *240*, 124412. https://doi.org/10.1016/j.ijbiomac.2023.124412

Budiarto, R., Wathoni, N., Mubarok, S., Hamdani, J. S., Ujilestari, T., Darsih, C., & Sholikin, M. M. (2024). Recent overview of Kaffir lime (*Citrus hystrix* DC) dual functionality in food and nutraceuticals. *Journal of Agriculture and Food Research*, *18*, 101384. https://doi.org/10.1016/j.jafr.2024.101384

Chattaviriya, P., Supawantanakul, D., Sangsirimongkolying, R., & Sua, I. G. (2022). Banana fibers as a sustainable acoustic absorbing material: A review. *Trends in Sciences, 19*(11), 4498. https://doi.org/10.48048/tis.2022.4498

Das, S., Das, M. K., Jamatia, T., Bhattacharya, B., Mazumder, R., Yadav, P. K., & Mandal, S. (2024). Advances of cassava starch based composites in novel and conventional drug delivery systems: A state of the art review. *RSC Pharmaceutics*, *1*(2), 182-203. https://doi.org/10.1039/d3pm00008g

Elisabeth, D. A. A., Utomo, J. S., Byju, G., & Ginting, E. (2022). Cassava flour production by small scale processors, its quality and economic feasibility. *Food Science and Technology, 42*, e41522. https://doi.org/10.1590/fst.41522

Ferdian, M. A., Perdana, R. G., & Rahardjo, P. P. (2023). Refinery technology of used cooking oil by utilizing coffee dregs and sugar cane bagasse as raw materials for making antiseptic transparent soap of guava leaf extract. *International Journal of Agriculture Environment and Food Sciences*, *7*(1), 11-20. https://doi.org/10.31015/jaefs.1109072

Freitas, P. A., Santana, L. G., González Martínez, C., & Chiralt, A. (2024). Combining subcritical water extraction and bleaching with hydrogen peroxide to obtain cellulose fibres from rice straw. *Carbohydrate Polymer Technologies and Applications*, *7*, 100491. https://doi.org/10.1016/j.carpta.2024.100491

Harun, S., & Geok, S. K. (2016). Effect of sodium hydroxide pretreatment on rice straw composition. *Indian Journal of Science and Technology, 9*(21), 1-9. https://doi.org/10.17485/ijst/2016/v9i21/95245

Hillscher, L. M., Höfler, M. V., Gutmann, T., Lux, C., Clerkin, K. U., Schwall, G., & Biesalski, M. (2024). Influence of TEMPO-oxidation on pulp fiber chemistry, morphology and mechanical paper sheet properties. *Cellulose*, *31*(5), 3067-3082. https://doi.org/10.1007/s10570-024-05748-5

Hosseini, M. H., Razavi, S. H., & Mousavi, M. A. (2009). Antimicrobial, physical and mechanical properties of chitosan-based films incorporated with thyme, clove and cinnamon essential oils. *Journal of Food Processing and Preservation*, *33*(6), 727-743. https://doi.org/10.1111/j.1745-4549.2008.00307.x

Islam, M., Sinha, A. S. K., & Prasad, K. (2024). Organosolv delignification of rice straw cellulose fiber for functional food packaging. *Cellulose*, *31*(15), 9191-9214. https://doi.org/10.1007/s10570-024-06125-y

Ketkaew, S., Kasemsiri, P., Hiziroglu, S., Mongkolthanaruk, W., Wannasutta, R., Pongsa, U., & Chindaprasirt, P. (2018). Effect of oregano essential oil content on properties of green biocomposites based on cassava starch and sugarcane bagasse for bioactive packaging. *Journal of Polymers and the Environment*, *26*, 311-318. https://doi.org/10.1007/s10924-017-0957-x

Kirillova, N. P., Vodyanitskii, Y. N., & Sileva, T. M. (2015). Conversion of soil color parameters from the Munsell system to the CIE Lab* system. *Eurasian Soil Science*, *48*(5), 468-475. https://doi.org/10.1134/S1064229315050026

Liu, S., Liu, X., Wang, Q., Wang, Y., Ji, X., Yang, G., & Ni, Y. (2022). Superhydrophobic, strong and transparent paper made from cellulosic fibers. *Cellulose*, *29*(3), 1993-2003. https://doi.org/10.1007/s10570-021-04393-6

Maimaiti, H., Arken, K., Wumaier, M., & Wushuer, L. (2014). Oil absorbency of cellulose/butylmethacrylate graft polymer fibers. *Iranian Polymer Journal*, *23*(9), 671-678. https://doi.org/10.1007/s13726-014-0261-8

Malik, K., Sharma, A., Harikarthik, D., Rani, V., Arya, N., Malik, A., Rani, S., Sangwan, P., & Bhatia, T. (2023). Deciphering the biochemical and functional characterization of rice straw cultivars for industrial applications. *Heliyon*, *9*(6), e16339. https://doi.org/10.1016/j.heliyon.2023.e16339

Malikhah, H., & Herdyastuti, N. (2023). Effect of kaffir lime (*Citrus hystrix*) leaf extract on xanthine oxidase inhibition. *World Journal of Advanced Research and Reviews*, *17*(1), 1069-1078. https://doi.org/10.30574/wjarr.2023.17.1.0100

Mazega, A., Tarrés, Q., Aguado, R., Pèlach, M. À., Mutjé, P., Ferreira, P. J., & Delgado Aguilar, M. (2022). Improving the barrier properties of paper to moisture, air, and grease with nanocellulose-based coating suspensions. *Nanomaterials*, *12*(20), 3675. https://doi.org/10.3390/nano12203675

Nagpal, R., Bhardwaj, N. K., Mishra, O. P., & Mahajan, R. (2021). Cleaner bio pulping approach for the production of better strength rice straw paper. *Journal of Cleaner Production*, *318*, 128539. https://doi.org/10.1016/j.jclepro.2021.128539

Paudel, B., Basak, J. K., Madhavi, B. G. K., Kim, N. E., Lee, G. H., Choi, G. M., & Kim, H. T. (2022). Properties of paper-based biodegradable pots for growing seedlings. *Horticulture, Environment, and Biotechnology*, *63*(6), 793-807. https://doi.org/10.1007/s13580-022-00457-z

Qi, J., Wang, X., Wang, X., Akoh, C. C., & Jin, Q. (2019). Effect of oil type and emulsifier on oil absorption of steam and fried instant noodles. *Journal of Oleo Science*, *68*(6), 559-566. https://doi.org/10.5650/jos.ess18217

Rahaman, A., Kumari, A., Zeng, X. A., Farooq, M. A., Siddique, R., Khalifa, I., Siddeeg, M. A., Ali, M., & Manzoor, M. F. (2021). Ultrasound-based modification and structural-functional analysis of corn and cassava starch. *Ultrasonics Sonochemistry*, *80*, 105795. https://doi.org/10.1016/j.ultsonch.2021.105795

Rahayu, M. S., Mellaratna, W. P., & Najah, N. (2024). The preliminary study on the antifungal effect of Kaffir lime (*Citrus hystrix* DC) peel extract against Malassezia furfur. *International Journal of Secondary Metabolite*, *11*(3), 486-493. https://doi.org/10.21448/ijsm.1395562

Ramadhan, D. S., Warsito & Iftitah, E. D. (2018). Microwave-assisted synthesis of benzimidazole derivatives from citronellal in kaffir lime (*Citrus hystrix* DC.) oil. *IOP Conference Series: Materials Science and Engineering*, *299*, 012048. https://doi.org/10.1088/1757-899X/299/1/012076

Rangappa, S. M., Siengchin, S., Parameswaranpillai, J., Jawaid, M., & Ozbakkaloglu, T. (2022). Lignocellulosic fiber reinforced composites: Progress, performance, properties, applications, and future perspectives. *Polymer Composites*, *43*(2), 645-691. https://doi.org/10.1002/pc.26413

Ray, A., Mohanty, S., Jena, S., Sahoo, A., Acharya, L., Panda, P. C., Sial, P., Duraisamy, P., & Nayak, S. (2022). Drying methods affect physicochemical characteristics, essential oil yield and volatile composition of turmeric (*Curcuma longa* L.). *Journal of Applied Research on Medicinal and Aromatic Plants*, *26*, 100357. https://doi.org/10.1016/j.jarmap.2021.100357

Risa, A. G., & Wolla, D. W. (2025). Characterization and finite element analysis of hybrid glass–maize stalk fibers–epoxy composite for bone plate application. *Fibers and Polymers*, *26,* 2543. https://doi.org/10.1007/s12221-025-00964-7

Rosdi, M. H. H. M., Ahad, N. A., & Shahdan, D. (2022). Comparison on oil and water absorption ability of various natural fiber. *Journal of Physics: Conference Series, 2169*(1), 012021. https://doi.org/10.1088/1742-6596/2169/1/012021

Sahu, O. (2021). Characterisation and utilization of heterogeneous catalyst from waste rice straw for biodiesel conversion. *Fuel*, *287*, 119543. https://doi.org/10.1016/j.fuel.2020.119543

Serrano-Martínez, V. M., Pérez-Aguilar, H., Carbonell-Blasco, M. P., Arán-Ais, F., & Orgilés-Calpena, E. (2024). Steam explosion based method for the extraction of cellulose and lignin from rice straw waste. *Applied Sciences*, *14*(5), 2059. https://doi.org/10.3390/app14052059

Sun, S., Xie, Y., Yang, R. J., Zhu, M. J., Sablani, S., & Tang, J. (2023). The influence of temperature and water activity on thermal resistance of Salmonella in milk chocolate. *Food Control*, *143*, 109292. https://doi.org/10.1016/j.foodcont.2022.109292

Todorova, D., Yavorov, N., Lasheva, V., Damyanova, S., & Kostova, I. (2022). Lavender essential oil as antibacterial treatment for packaging paper. *Coatings*, *13*(1), 32. https://doi.org/10.3390/coatings13010032

Toro, R. G., Diab, M., de Caro, T., Al Shemy, M., Adel, A., & Caschera, D. (2020). Study of the effect of titanium dioxide hydrosol on the photocatalytic and mechanical properties of paper sheets. *Materials*, *13*(6), 1326. https://doi.org/10.3390/ma13061326

Wang, F. J., Wang, L. Q., Zhang, X. C., Ma, S. F., & Zhao, Z. C. (2022). Study on the barrier properties and antibacterial properties of cellulose-based multilayer coated paperboard used for fast food packaging. *Food Bioscience*, *46*, 101398. https://doi.org/10.1016/j.fbio.2021.101398

Wembe, B. D., Djomi, R., Konai, N., Ntamack, G. E., Tsopmo, F. A., Olubusoye, O. E., & Mevaa, L. (2023). Investigation on the mechanical properties of paper water hyacinth (Eichhornia crassipes). *European Journal of Engineering and Technology Research*, *8*(1), 54-58. https://doi.org/10.24018/ejeng.2023.8.1.2965

Wichianphong, N., & Maison, W. (2020). Preparation of biofuel pellets from water hyacinth and waste coffee grounds. *RMUTSB Academic Journal*, *8*(2), 140-152. https://li01.tci-thaijo.org/index.php/rmutsb-sci/article/view/247484

Wu, T., Wang, X., & Inada, T. (2025). Research on hydroponic cultivation substrates made from rice straw. *Sustainability*, *17*, 772. https://doi.org/10.3390/su17020772

Xing, T., Dong, C., Hu, X., Zheng, Q., Zhang, J., Zhao, Y., & Wang, X. (2024). Cellulose membranes via a top-down approach from loofah for oil/water separation. *Biomass Conversion and Biorefinery*, *14*(15), 17167-17175. https://doi.org/10.1007/s13399-023-03766-0

Xu, L. P., Dai, B., Fan, J., Wen, Y., Zhang, X., & Wang, S. (2015). Capillary-driven spontaneous oil/water separation by superwettable twines. *Nanoscale, 7*(31), 13164-13167. https://doi.org/10.1039/C5NR03670D

Yang, Q., Ruan, F., Wu, H., Kan, C., Wang, G., Wang, Z., & Wang, H. (2023). Effect of chemical treatment on rice straw fiber surface and properties of straw/polylactic acid composites. *Journal of Natural Fibers*, *20*(2), 2228486. https://doi.org/10.1080/15440478.2023.2228486

Yimlamai, P., Chitbanyong, K., Wanitpinyo, K., Puangsin, B., Nanta, K., Khantayanuwong, S., Pisutpiched, S., Chaisan, T., Fei, B., & Hiziroglu, S. (2024). Properties of mixture of hemp bast and softwood pulp for filter paper manufacture. *Heliyon*, *10*(3), e24125. https://doi.org/10.1016/j.heliyon.2024.e25353

Ying, N. H., Min, G. S., & Asman, S. (2023). Extraction of essential oil *Citrus hystrix* by using ultrasound assisted extraction. *Malaysian Journal of Analytical Sciences*, *27*(6), 1236-1248. https://mjas.analis.com.my/mjas/v27_n6/pdf/Ying_27_6_6.pdf

Zaafarani, N. N., Nour, M., El Kassas, A. M., & Elsheikh, A. (2024). A new recycled high impact polystyrene rice straw composite: Eco-friendly fabrication and characterization. *International Journal of Environmental Science and Technology*, *21*(2), 1193-1202. https://doi.org/10.1007/s13762-023-05039-9

Zhang, Y., Sam, E. K., Liu, J., & Lv, X. (2023). Biomass based/derived value added porous absorbents for oil/water separation. *Waste and Biomass Valorization*, *14*(10), 3147-3168. https://doi.org/10.1007/s12649-023-02112-9